Iranian Journal of Medical Physics

ijmp.mums.ac.ir

Tumor and Critical Organ Dose Assessment in Parotid Gland Radiotherapy: Comparison of Calculated and Measured Dose Using Different Techniques

Mohammad Taghi Bahreyni Toossi[1], Hamid Gholamhosseinian[2], Kazem Anvari[3], Bahar Zargari[4], Atefeh Vejdani Noghreiyan[5] *

1. Medical Physics Research Centre, Mashhad University of Medical Sciences, Mashhad, Iran
2. Department of Medical Physics, School of Medicine, University of Medical Sciences, Mashhad, Iran
3. Department of Radiotherapy Oncology, Omid Hospital, Cancer Research Center, School of Medicine Mashhad University of Medical Sciences, Mashhad, Iran
4. Student Research Committee, Babol University of Medical Sciences, Babol, Iran
5. Cancer Research Center, Health Research Institute, Babol University of Medical Sciences, Babol, I.R.Iran.

ARTICLE INFO

Article type:
Original Paper

Article history:
Received: Sep 14, 2025
Accepted: Dec 25, 2025

Keywords:
Parotid Tumor
Radiotherapy
Tumor Dose
TLD
Rando Phantom

ABSTRACT

Introduction: Parotid gland tumors account for approximately 3% of head and neck malignancies. Surgery is the primary treatment modality, while postoperative radiotherapy is recommended for high-grade tumors to reduce local recurrence. Several radiotherapy techniques have been used for postoperative parotid irradiation, each with different dosimetric characteristics. Among the most common approaches are angled wedged photon beams and ipsilateral mixed photon–electron beams. This study aimed to compare commonly used parotid radiotherapy techniques dosimetrically and propose clinical optimization strategies.

Material and Methods: A head-and-neck anthropomorphic Rando phantom was scanned using computed tomography with 5-mm slice thickness. Imaging data were transferred to the Isogray treatment planning system (TPS). Target volume and organs at risk (OARs) were contoured, and thermoluminescent dosimeters (TLDs) were used for dose measurements. Three radiotherapy techniques were evaluated regarding dose homogeneity, target coverage, organ sparing, and agreement between calculated and measured doses.

Results: Wedged-pair photon techniques with and without multileaf collimator (MLC) showed better dose homogeneity within the planning target volume (PTV) than the mixed photon–electron technique ($\Delta D_{5\%}-D_{95\%}$: 2.31 and 2.28 Gy vs 6.14 Gy). The MLC-based wedged-pair technique provided superior sparing of tissues beyond the target volume, while the mixed beam technique resulted in the lowest oral cavity dose (1.9 Gy). All techniques achieved at least 95% PTV coverage. Measured and calculated doses showed acceptable agreement, although some discrepancies were observed in heterogeneous regions such as the mandible.

Conclusion: No single radiotherapy technique was optimal for all dosimetric objectives. Combining techniques may improve normal tissue sparing while maintaining adequate and homogeneous tumor dose coverage.

► *Please cite this article as:*
Bahreyni Toossi MT, Gholamhosseinian H, Anvari K, Zargari B, Vejdani Noghreiyan A. Tumor and Critical Organ Dose Assessment in Parotid Gland Radiotherapy: Comparison of Calculated and Measured Dose Using Different Techniques. Iran J Med Phys 2026; 23 (1): 1-8. 10.22038/ijmp.2026.90428.2598.

Introduction

Parotid gland tumors represent approximately 3% of head and neck malignancies. Surgery remains the cornerstone of treatment, while adjuvant radiotherapy is recommended for high-grade tumors, positive margins, perineural invasion, or nodal involvement [1, 2].

The anatomical proximity of the parotid gland to critical structures such as the spinal cord, brainstem, mandible, and oral cavity presents a significant dosimetric challenge. Therefore, achieving adequate target coverage while minimizing radiation-induced toxicity remains a major clinical concern.

Conventional radiotherapy techniques for superficial head and neck tumors include wedged-pair photon beams and mixed photon–electron beams [3]. Electron beams, due to their finite range, can provide favorable dose distributions for superficial targets; however, dose inhomogeneity and hot spots may occur when target depth varies.

Advances in conformal radiotherapy, particularly techniques utilizing multileaf collimators (MLC), have improved dose conformity and homogeneity compared with those of conventional electron or mixed-beam techniques [4-6]. Furthermore, intensity-modulated radiotherapy (IMRT) and volumetric modulated arc therapy (VMAT) have demonstrated superior sparing of salivary glands and other critical structures [7-9].

**Corresponding Author:* Email: a.vejdani@mubabol.ac.ir

Nutting et al. demonstrated that three-dimensional conformal radiotherapy resulted in a significant reduction in radiation dose to critical normal tissues compared with conventional radiotherapy, while IMRT achieved an additional reduction in the dose delivered to the cochlea and oral cavity.

Despite the availability of advanced treatment techniques, many radiotherapy centers continue to rely on conventional wedged photon and mixed photon–electron techniques due to equipment limitations and clinical workflow considerations.

Moreover, the optimal choice of technique for parotid gland irradiation remains a subject of debate, particularly when balancing target dose homogeneity against protection of adjacent organs at risk. Therefore, a dosimetric evaluation of commonly used techniques remains clinically relevant. The present study aimed to compare three widely used parotid gland radiotherapy techniques using experimental dose measurements and to identify potential optimization strategies applicable in routine clinical practice.

Materials and Methods

Phantom and Treatment Planning

An anthropomorphic Alderson–Rando phantom was used to simulate a patient with a parotid gland tumor. CT images were acquired with a 3-mm slice thickness, and the data were transferred to the Isogray treatment planning system.

Target volume and surrounding organs at risk (OARs) were contoured on each CT slice. The delineated structures included the parotid tumor, penumbra, contralateral parotid gland, spinal cord, mandible, brain stem, left cochlea, right cochlea, and oral cavity. A uniform 5-mm margin was added to the clinical target volume to generate the PTV, in accordance with RTOG-1008 recommendations.

Normal tissue dose constraints were evaluated based on the QUANTEC guidelines and subsequent updates [10, 11].

Treatment Techniques

Three techniques were evaluated:

1. Mixed photon–electron beam (6 MV photon + 10 MeV electron, 1:2 weighting)
2. Ipsilateral wedged-pair photon beams (6 MV)
3. Ipsilateral wedged-pair photon beams with MLC (6 MV)

Dosimetry and TLD Calibration

Lithium fluoride TLD-700 chips were used for dose measurements. Calibration procedures followed standard protocols, including element correction coefficient (ECC) and reader calibration factor (RCF) determination. Separate calibration curves were obtained for photon and electron beams.

Lithium fluoride thermoluminescent dosimeters (TLDs) with a cross-sectional area of 3 × 3 mm² and a thickness of 0.9 mm (TLD-700, Harshaw-Bicron) were employed to assess the dose received by the tumor and critical organs [12]. TLD readings were obtained using a 3500 TLD reader (Harshaw-Bicron). Prior to irradiation, the TLDs underwent annealing at 400 ºC for 1 hour followed by 100 ºC for 2 hours. The calibration of the TLDs consisted of three steps, with the first stage involving the determination of the ECC coefficients. The second stage of calibration, RCF (Reader Correction Factor) for the TLD reader device was obtained. The RCF coefficient of the TLD-Reader device was calculated using TLD reader software (WinREMS):

$$RCF = \frac{\langle Q \rangle}{L} \quad (1)$$

Where <Q> is the mean charge of the dosimeter and L is the dose value which dosimeters are irradiated.

Finaly, the third stage of ECC for each dosimeter was obtained obtained.

$$ECCj = \frac{\langle Q \rangle}{qj} \quad (2)$$

Here, ECCj_jj represents the correction factor for the jjjth dosimeter, <Q> is the average charge of all dosimeters, and qjq_jqj is the measured charge of the jjjth dosimeter. Each dosimeter was calibrated prior to being placed in the TLD reader system. This calibration aimed to determine a thermoluminescent (TL) efficiency correction factor for each dosimeter element [13]. The TLDs were subsequently divided into two groups. One group of TLDs was calibrated with 6MV photon and another group was calibrated with 6 MeV electron. The calibration dosimeters were irradiated with 0.7, 1.0, 1.3, 1.5, 1.7, and 2.0 Gy doses and linearity region of TLDs response was determined. TLD doses up to 1.3 Gy showed supralinear response; therefore, the delivered dose to the TLDs for the three techniques was kept below 1.3 Gy.

Statistical Analysis

Statistical analyses were conducted using SPSS version 21. The normality of the data was assessed with the Kolmogorov–Smirnov test. Independent t-tests were used to compare dose differences between techniques, with a significance threshold of $p < 0.05$.

Ethical Considerations

- This experimental phantom study did not involve human subjects or patient data and, as a result, did not require approval from an institutional review board.

Dosimetric comparison of three radiotherapy techniques of parotid gland tumors

Comparison of three radiotherapy techniques based on the absorbed dose to the target volume and surrounding organs at risk was performed using thermoluminescent dosimeters (TLDs). The nominal prescribed dose to the planning target volume was 60.0 Gy delivered in 30 fractions, using an Elekta linear accelerator.

To increase the accuracy and reproducibility of the measured doses in the target volume and critical structures, each radiotherapy technique was independently delivered three times, and the average measured values were used for dosimetric evaluation.

For all three techniques, the head and neck region of the phantom was positioned laterally on the treatment couch. Reproducibility of the setup was ensured by aligning the treatment room lasers with reference marks placed on the phantom during the CT simulation, thereby maintaining identical positioning between CT scanning and irradiation sessions.

Within the mixed photon–electron beam technique, three different photon-to-electron weightings (1:2, 1:3, and 1:4) were investigated using the treatment planning system in order to evaluate their effects on dose distribution, target dose homogeneity, and hotspot formation.

For the mixed photon–electron beam technique, prior to photon irradiation, TLDs calibrated for 6 MV photon beams were embedded at predefined locations within the phantom. The phantom was then irradiated with 6 MV photons, delivering a dose of 1 Gy to the depth of maximum dose (Dmax) at a source-to-surface distance (SSD) of 100 cm, using a 1-cm tissue-equivalent bolus over the treatment region (Figure 1).

Figure1. The pattern of irradiating with photon, Linac accelerator (Elekta–Precise)

Following photon irradiation in the mixed beam technique, electron irradiation was performed using 10 MeV electron beams. The electron field was designed to adequately cover the superficial component of the target volume while minimizing the dose to deeper normal tissues (Figure 2).

The electron beam was delivered using an applicator with an appropriate field size, and beam shaping was achieved to conform to the planning target volume. The same TLD positions used for photon irradiation were maintained to ensure consistency in dose measurement across all techniques.

Figure 2. The pattern of irradiating with photon, Linac accelerator (Elekta–Precise)

For wedged-pair photon techniques, treatment plans were generated using two ipsilateral 6 MV photon beams with appropriate wedge angles to improve dose uniformity within the target volume. In one approach, conventional wedged-pair fields were used, while in the other approach, multileaf collimators (MLCs) were applied to further conform the dose to the target and reduce irradiation of adjacent normal tissues, as shown in Figure 3.

Figure 3.The pattern of ipsilateral wedged-pair technique using 6 MV photon and MLC, Linac accelerator (Elekta–Precise)

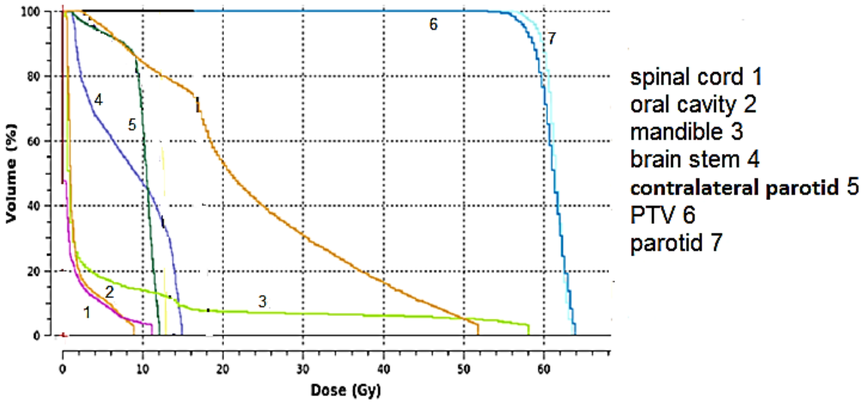

Figure 4. The DVH of mixed beam technique of photon and electron

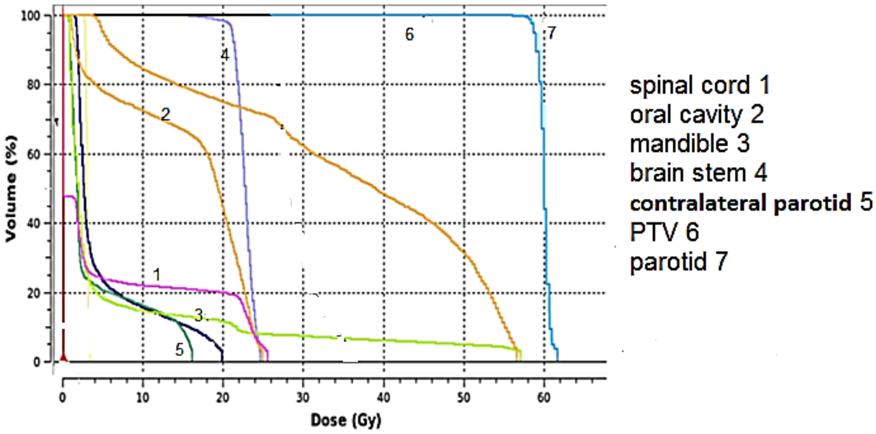

Figure 5. The DVH of wedged-pair technique using photon

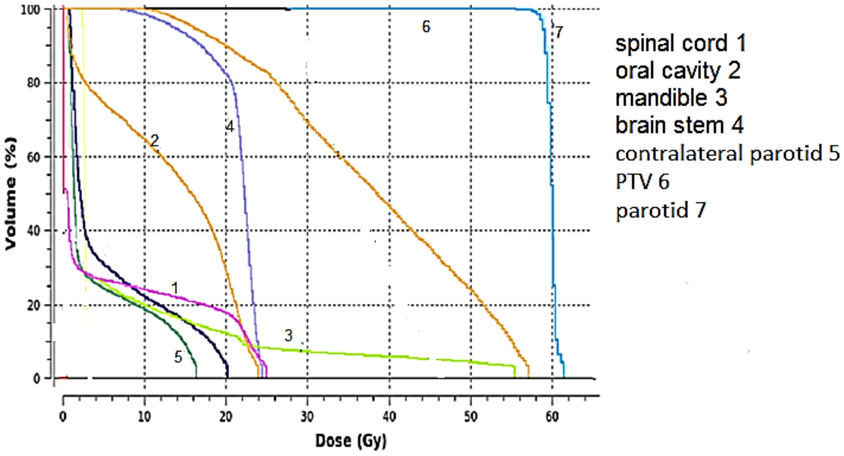

Figure 6. The DVH of wedged-pair technique using photon and MLC

All treatment plans were created on the same treatment planning system using identical CT datasets and structure delineations to ensure a fair comparison between techniques. Dose calculations were performed using the system's clinical algorithm, and dose distributions were evaluated in terms of target coverage, dose homogeneity, and dose to organs at risk. TLD chips were placed at representative locations within the planning target volume, mandible, spinal cord, brain stem, contralateral parotid gland, oral cavity, and penumbra region. After irradiation, TLDs were read out under standardized conditions, and the measured doses were compared with the corresponding calculated doses from the treatment planning system. Dosimetric comparison between the three radiotherapy techniques was performed based on mean and maximum doses to the target volume and critical structures, as well as dose homogeneity indices and agreement between measured and calculated doses.

To achieve a homogenous dose, 40-degree wedge and 45, 50 degree wedges were used for technique [2] and technique [3], respectively. For technique [3], the margin of the leaves of the MLCs was 3-8 mm.

Normal Tissues Tolerance is based on the QUANTEC [27, 28].

Statistical analysis

A statistical package for social sciences (SPSS, version 21.0) software was employed to calculate the mean absorbed doses received to tumor and critical structures surrounding.

One -Sample Kolmogrov-Smirnov Test indicated that all the data had a normal distribution;

To analyze the dose difference (in PTV, penumbra, contralateral parotid, spinal cord and mandible) between three techniques, independent T-test was performed.

This study did not involve human participants, their data, or biological material. Therefore, in accordance with applicable ethical standards, including the 1964 Declaration of Helsinki and its later amendments, this research was exempt from Institutional Review Board (IRB) approval, as it did not involve any human subjects.

Results

Investigation of photon-to-electron weightings in the mixed-beam technique

Three different photon-to-electron weightings were evaluated using 6-MV photons and 10-MeV electrons. The maximum dose for the 1:2, 1:3, and 1:4 photon-to-electron weightings was 64.06 Gy, 64.69 Gy, and 65.11 Gy, respectively. All three weightings resulted in doses to critical organs below tolerance limits, with no statistically significant superiority observed among them. However, the 1:2 photon-to-electron weighting produced the lowest hotspot dose within the target volume and was therefore selected for further dosimetric measurements.

Tumor and organs-at-risk dose

Dose homogeneity within the target volume was assessed using the inhomogeneity index (IHI), defined as the difference between D5% and D95%. Lower IHI values indicate improved dose uniformity. The IHI values for the three techniques are presented in Table 1.

Table 1. shows the IHI values for three techniques.

Techniques	IHI (Gy)
The mixed beam of photon and electron	6.14
wedged-pair technique using photon	2.31
wedged-pair technique using photon and MLC	2.28

The mixed photon–electron technique demonstrated the highest IHI value (6.14 Gy), indicating poorer dose homogeneity compared with the wedged-pair photon technique (2.31 Gy) and the wedged-pair photon technique using MLC (2.28 Gy).

These findings confirm that wedged-pair photon techniques provide superior target dose homogeneity compared with mixed-beam irradiation.

Measured absorbed doses to the target volume and critical structures are summarized in Table 2. All techniques delivered at least 95% of the prescribed dose to the PTV. Differences in measured doses to the mandible, spinal cord, contralateral parotid gland, and penumbra were not statistically significant ($p > 0.05$).

In contrast, significant differences were observed in the PTV dose between the mixed-beam technique and both wedged-pair techniques ($p < 0.05$).

For uniform dose coverage to the prescription depth, the inhomogeneity index (IHI) was assessed depending on the technique used. The lower IHI value, the more homogeneity in target volume is achieved.

The differences among the measured doses by TLDs for the mandible, spinal cord, contralateral parotid gland, and penumbra were not statistically significant across the three treatment techniques ($p > 0.05$). For the PTV, however, the mixed beam of photon and electron technique differed significantly from wedged-pair technique using photon technique and wedged-pair technique using photon and MLC technique (p-value< 0.05).

Comparison between calculated and measured dose

To evaluate the agreement between treatment planning system (TPS) calculations and TLD measurements, the relative deviation (δ) was calculated. According to the TRS-430 protocol, acceptable deviations are <4% for inner-field points and <40% for outer-field and complex geometry regions.

As shown in Table 3, most measurement points demonstrated acceptable agreement between calculated and measured doses for all three techniques. Larger deviations were mainly observed in regions with steep dose gradients or tissue heterogeneities, such as the mandible and contralateral parotid gland.

In order to compare the measured dose by TLD and the calculated dose by the treatment planning system, δ was used to determine the deviation between the individual calculated and measured points. The relative deviation was defined as:

$$\delta = \left(\frac{Dcal - Dmeas}{Dmeas}\right) \times 100 \qquad (3)$$

Where D_{cal} is the calculated dose and D_{meas} is the measured dose. Based on the Technical Reports Series 430, the tolerances of δ is less than 40% for outer of the field, complex geometry, wedge fields, heterogeneity and asymmetry and is less than 4% for the inner part of the field [14].

$\boldsymbol{\delta}_1$, $\boldsymbol{\delta}_2$ and $\boldsymbol{\delta}_3$ are the percentage of relative tolerance for the mixed beam technique using 6 MV photon and 10 MeV electron (1:2 weighting), the ipsilateral wedged-pair technique using 6 MV photon and the ipsilateral wedged-pair technique using 6 MV photon and MLC .

Table 3 shows the percentage of deviation between the results of TLD measurement and those calculated by the treatment planning system for three therapeutic techniques.

Table 2 shows the measured dose of the target volume and critical structures for three radiation therapy techniques of parotid tumor.

Brain stem (percentage of dose receiving)	Oral cavity (percentage of dose receiving)	contralateral parotid (mean)	spinal cord (mean)	Mandible (mean)	PTV (mean)	penumbra (mean)	Techniques
%26.83	%3.37	13.77± 1.28	1.01 ± 0.17	1.85± 1.39	65.93± 2.71	57.35± 4.41	The mixed beam of photon and electron
%38.06	% 31.95	8.14 ± 9.43	1.61 ± 0.57	1.73± 0.53	62.01± 1.94	54.67± 6.73	wedged-pair technique using photon
%32.46	%29.88	9.92 ± 8.46	1.54± 0.5	1.76± 0.45	58.53 ±1.73	47.26± 14.88	wedged-pair technique using photon and MLC

Table 3. The percentage of deviation between the results of Dmeas and Dcal for target volume and critical organs.

δ3	$\boldsymbol{\delta}_2$	$\boldsymbol{\delta}_1$	
%-43.66	%-44.44	%-26.43	Mandible
%-22.33	%-10.42	%-40.14	
%8.42	%2.08	%-11.6	Oral cavity
%0.66	%-11.29	%-23.6	Brain stem
%-32.20	%-16.66	%-37.07	spinal cord
%-53.15	%-0.99	%-20.35	
%65.01	%6.00	%10.14	contralateral parotid
%-40.54	%-3.10	%-14.60	
%-3.15	%-3.23	%-12.67	
%1.24	%-3.23	%5.61	PTV
%4.30	%1.26	%3.93	
%3.06	%-3.91	%-4.91	
%-1.53	%-4.75	%-4.51	

Discussion

In this study, we compared the absorbed dose to the planning target volume (PTV) and surrounding organs at risk using three different radiotherapy techniques for parotid gland tumors. In addition, the agreement between calculated doses obtained from the treatment planning system and experimentally measured doses using thermoluminescent dosimeters (TLDs) was investigated in order to evaluate the dosimetric accuracy of each technique.

As shown in Table 1, the ipsilateral wedged-pair techniques using 6 MV photons, both with and without multileaf collimators (techniques [2] and [3]), demonstrated significantly improved dose homogeneity within the PTV, with inhomogeneity index (IHI) values of 2.31 Gy and 2.28 Gy, respectively, compared with the mixed photon–electron technique (technique [1]), which exhibited a higher IHI value of 6.14 Gy. This finding indicates superior dose uniformity in the target volume when photon wedged-pair techniques are employed.

Despite differences in dose homogeneity, all three techniques provided adequate target coverage, with at least 95% of the prescribed dose delivered to the PTV. This confirms that each technique is clinically acceptable in terms of basic target coverage requirements.

Evaluation of penumbra doses revealed that the wedged-pair technique using 6 MV photons with MLCs resulted in the greatest dose reduction to normal tissues adjacent to the PTV. This improvement can be attributed to enhanced beam conformity achieved through MLC shaping, which limits dose spillage outside the target volume and reduces irradiation of contiguous normal structures.

Late radiation-induced toxicities following conventional radiotherapy of salivary gland and parotid tumors include xerostomia, hearing impairment, soft tissue fibrosis, taste alteration, and dental complications. Reducing the dose to adjacent normal tissues, particularly the contralateral parotid gland and oral cavity, is therefore of major clinical importance. Our findings suggest that the ipsilateral wedged-pair technique using 6 MV photons with MLCs is more effective in minimizing dose to these structures compared with the mixed photon–electron technique, potentially reducing the risk of such late side effects [7, 8].

Dose–volume histograms (DVHs) for organs at risk are presented in Figures 4–6. DVH analysis showed that, for the brain stem, the volume receiving doses ≤ 59 Gy (1–10 cm³) remained below tolerance levels for all three techniques, corresponding to a less than 5% probability of necrosis or cranial neuropathy, in accordance with QUANTEC recommendations [10]. The mixed photon–electron technique demonstrated the lowest brainstem dose among the evaluated techniques. For the spinal cord, the maximum dose remained well below the accepted tolerance limit of 50 Gy for all techniques, indicating a negligible risk of radiation-induced myelopathy. Similarly, the mean dose to the oral cavity was below 50 Gy in all treatment approaches, suggesting a low probability of PEG tube–dependent aspiration, with the mixed beam technique yielding the lowest oral cavity dose [10].

The parotid glands are among the most radiosensitive organs in head and neck radiotherapy. Excessive irradiation can lead to severe xerostomia and permanent salivary dysfunction. According to established dose–response data, maintaining the mean dose to a single parotid gland below 20 Gy significantly reduces the risk of Grade 4 xerostomia. In the present study, the mean dose to the contralateral parotid gland remained below this threshold for all three techniques, suggesting a low probability of severe xerostomia following treatment.

Our results are consistent with previous studies, including those by Nutting et al., which demonstrated improved sparing of normal tissues and enhanced dose conformity using advanced photon-based techniques compared with conventional approaches [7, 8]. Unlike many previous investigations that relied solely on treatment planning system calculations, the present study incorporated direct dose measurements using TLDs, providing experimental validation of the calculated dose distributions.

A notable discrepancy between calculated and measured doses was observed in the mandible. In general, the treatment planning system tended to overestimate the absorbed dose compared with TLD measurements. Similar discrepancies have been reported by Ostwald et al., particularly in regions characterized by steep dose gradients and tissue density heterogeneities, such as bone–soft tissue interfaces. These findings highlight the limitations of dose calculation algorithms in regions of rapid dose fall-off.

Overall, based on the TRS-430 protocol, more than 95% of measured dose points, both inside and outside the radiation field, were in acceptable agreement with calculated doses for all three techniques, confirming the overall reliability of the treatment planning system.

Conclusion

This study demonstrates that different radiotherapy techniques for parotid gland tumors exhibit distinct dosimetric characteristics. While the mixed photon–electron technique provides reduced doses to certain organs at risk, the ipsilateral wedged-pair photon techniques, particularly when combined with MLCs, offer superior dose homogeneity within the PTV and improved sparing of adjacent normal tissues.

The incorporation of MLCs in photon wedged-pair techniques appears to be especially advantageous in reducing penumbra dose and limiting irradiation of structures adjacent to the target volume. Furthermore, experimental dose verification using TLDs confirms the general accuracy of treatment planning system calculations, while also highlighting areas where calculation uncertainties may arise.

In clinical practice, the selection of an optimal radiotherapy technique should consider both target dose homogeneity and protection of critical structures. When available, the wedged-pair technique using 6 MV photons with MLCs may be preferred for parotid gland tumors to minimize late radiation-induced complications while maintaining adequate target coverage.

Acknowledgment

The authors would like to express their sincere appreciation to Mashhad University of Medical Sciences for the financial support of this research. The authors also thank the Radiotherapy Department of Emam Reza Hospital for providing access to the linear accelerator and treatment planning system, as well as the Medical Physics Research Center for supporting this study through the use of the TLD reader system.

References

1. Yaparpalvi R, Fontenla DP, Tyerech SK, Boselli LR, Beitler JJ. Parotid gland tumors: a comparison of postoperative radiotherapy techniques using three dimensional (3D) dose distributions and dose-volume histograms (DVHS). Int J Radiat Oncol Biol Phys. 1998;40(1):43-9.
2. Vejdani Noghreiyan V, Naseri S, Momennezhad M. Utilization of Electronic Portal Imaging Device (EPID) For Setup Verification and Determination of Setup Margin in Head and Neck Radiation Therapy. Iranian Journal of Medical Physics. 2020;17(3):197-204.
3. Blasi O, Fontenot JD, Fields RS, Gibbons JP, Hogstrom KR. Preliminary comparison of helical tomotherapy and mixed beams of unmodulated electrons and intensity modulated radiation therapy for treating superficial cancers of the parotid gland and nasal cavity. Radiat Oncol. 2011;6:178.
4. Cozzi L, Fogliata A, Bolsi A, Nicolini G, Bernier J. Three-dimensional conformal vs. intensity-modulated radiotherapy in head-and-neck cancer patients: comparative analysis of dosimetric and technical parameters. Int J Radiat Oncol Biol Phys. 2004;58(2):617-24.
5. Soleymanifard S, Toossi MT, Khosroabadi M, Noghreiyan AV, Shahidsales S, Tabrizi FV. Assessment of skin dose modification caused by application of immobilizing cast in head and neck radiotherapy. Australas Phys Eng Sci Med. 2014;37(3):535-40.
6. Kudchadker RJ, Hogstrom KR, Garden AS, McNeese MD, Boyd RA, Antolak JA. Electron conformal radiotherapy using bolus and intensity modulation. Int J Radiat Oncol Biol Phys. 2002;53(4):1023-37.
7. Nutting CM, Rowbottom CG, Cosgrove VP, Henk JM, Dearnaley DP, Robinson MH, et al. Optimisation of radiotherapy for carcinoma of the parotid gland: a comparison of conventional, three-dimensional conformal, and intensity-modulated techniques. Radiother Oncol. 2001;60(2):163-72.
8. Nutting CM, Morden JP, Harrington KJ, Urbano TG, Bhide SA, Clark C, et al. Parotid-sparing intensity modulated versus conventional radiotherapy in head and neck cancer (PARSPORT): a phase 3 multicentre randomised controlled trial. Lancet Oncol. 2011;12(2):127-36.
9. Mali SB. Adaptive Radiotherapy for Head Neck Cancer. J Maxillofac Oral Surg. 2016;15(4):549-54.
10. Emami B, Lyman J, Brown A, Coia L, Goitein M, Munzenrider JE, et al. Tolerance of normal tissue to therapeutic irradiation. Int J Radiat Oncol Biol Phys. 1991;21(1):109-22.
11. Bentzen SM, Constine LS, Deasy JO, Eisbruch A, Jackson A, Marks LB, et al. Quantitative Analyses of Normal Tissue Effects in the Clinic (QUANTEC): an introduction to the scientific issues. Int J Radiat Oncol Biol Phys. 2010;76(3 Suppl):S3-9.
12. Bahreyni TMT, Gholamhosseinian H, Vejdani NA. Assessment of the Effects of Radiation Type and Energy on the Calibration of TLD-100. 2018.
13. Luo L. Extensive fade study of Harshaw LiF TLD materials. Radiation Measurements - RADIAT MEAS. 2008;43:365-70.
14. Van Dyk J. QA of computerized radiation treatment planning systems. Book of Extended Synopses. 2006:214.